River Flow 2010 - Dittrich, Koll, Aberle & Geisenhainer (eds) - © 2010 Bundesanstalt für Wasserbau ISBN 978-3-939230-00-7

Lagrangian Block Hydrodynamics of Macro Resistance in a River-Flow Model

Lai Wai Tan & Vincent H. Chu
Department of Civil Engineering, McGill University, Montreal, Quebec H3A 2K6, Canada

ABSTRACT: A Lagrangian block hydrodynamics model has been developed for the computation of high speed river flow in steep channel during the flood stage. The model captures the depth-and-velocity discontinuities across the hydraulic jumps and the advance and retreat of water over the dry bed accurately with absolute computational stability. Turbulence simulations for a high speed river-flow model are carried out to demonstrate the stability of the computational model. The macro flow resistance of the turbulent shear flow is determined over a range of Froude number varying from Fr = 0.45 to 6.62.

Keywords: Lagrangian block hydrodynamics, High-speed river flow, Macro resistance, Flood waves

1 INTRODUCTION

Numerical simulation of high speed flow on steep channel is important for the study of sediment transport in the upstream rivers of steep slope (AGU Monograph 110, 1999). The lifting of large rocks and boulders at flood stage often is the consequence of the shock waves (hydraulic jumps) of high turbulent intensity interacting with the movable bed. Bank erosion causes the migration of sediments from the shore to the main stream. Resettlement of sediments on shore occurs in recirculating flow region behind large scale feature of the shore (Webb et al. 1999). The lateral turbulence exchanges can be determined by reliable computational model. The computation must not collapse as the water negotiates through the large scale and complex features of the channel. It must be able to capture the depth-and-velocity discontinuity across the shock waves. It must also allow the water to advance and retreat over the dry river bed.

The classical computational fluid dynamics are based on the estimate of fluxes on the faces of the finite volume. In the computation of waves and turbulence in shallow waters, the use of a truncated series to estimate the fluxes can lead to spurious numerical oscillations, negative water depth and the subsequent collapse of the computations. Such numerical instability problem is most severe in regions across the shock waves and at the advancing-and-retreating fronts of water over dry river bed. Chu and Altai (2001, 2002) used blocks of fluid and Lagrangian advection of the blocks to conduct simulations in a stream-function and vorticity formulation. Tan and Chu (2009a,b, 2010) applied the Lagrangian block hydrodynamics (LBH) method for one-dimensional (1D) simulation of the waves in shallow-waters using the primitive variable formulation. Other Lagrangian methods such as the method of the particle-in-cell (PIC) of Harlow (1964) and the method of the smoothed particle hydrodynamics (SPH) of Monaghan (2005) use artificial particles. The LBH method uses the real fluid blocks as the computational elements. Therefore, the kernel function used to calculate the interaction force between the artificial particles in SPH is not required. In this paper, the 1D LBH method of Tan and Chu (2009a, b, 2010) is extended for application to two-dimension (2D) problems and is applied to flood routing. Calculations are conducted using the LBH model to determine the advance-and retreat of water on dry bed and the macro flow resistance in supercritical and subcritical turbulent streams over a wide range of Froude number.

2 LAGRANGIAN BLOCK HYDRODYNAMICS

The Lagrangian blocks are arrays of contiguous fluid elements. The transfer of mass and the momentum in the fluid are carried out in the computation by staggered systems of blocks. Figure 1(a) shows the staggered grid and the relative locations of the volume block ($h\Delta x\Delta y$), and the x- and y-momentum blocks [($\rho uh\Delta x$), ($\rho vh\Delta y$)] on the grid. The x- and y-components of the velocity are defined at a distance of ½ Δx to the west and ½ Δy to the south of the water depth node, respectively. Figure 1(b) shows the advection of the volume block and Figs. 1(c) and 1(d) show the advection of the momentum blocks. A block of water for Lagrangian advection is defined by its water depth $h^L{}_i$ and the blocks widths $x^L{}_{i+1} - x^L{}_i = \Delta x^L$ and $y^L{}_{i+1} - y^L{}_i = \Delta y^L$. At the beginning of the Lagrangian advection, at time t, the blocks fit the Eulerian mesh, that is $x^L{}_i = x_i$ and $y^L{}_i = y_i$. At the end of the advection step, at time $t + \Delta t$, $\Delta x^L \Delta y^L h^L{}_i = \Delta x_i \Delta y_i h_i$ for volume conservation.

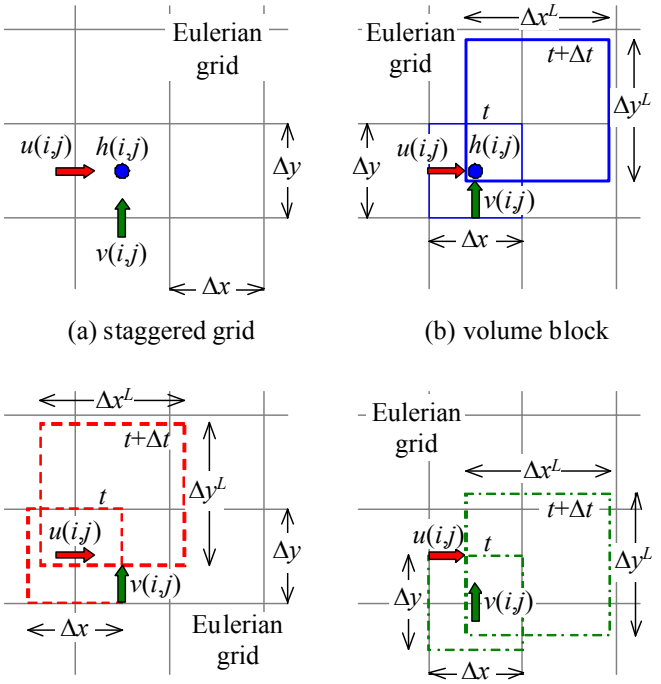

Figure 1. (a) The staggered water depth and velocity nodes on the Eulerian grid, (b) the volume block, (c)-(d) the x- and y-momentum blocks at the beginning and the end of a Lagrangian advection time step.

The mass and the momentum in the blocks are re-casted onto the Eulerian mesh at each computational time step. For the flood waves in shallow water, the forces on the blocks are calculated by assuming hydrostatic pressure variation over the depth. The edge positions of the blocks $x^L{}_i$ and $y^L{}_i$ at time $t + \Delta t$ are calculated by Lagrangian integration of the momentum equations:

$$\frac{Du^L{}_i}{Dt} = -g\frac{h_i - h_{i-1}}{\Delta x} - g\left(S_{ox} - S_{fx}\right) \quad (1)$$

$$\frac{Dv^L{}_i}{Dt} = -g\frac{h_i - h_{i-1}}{\Delta y} - g\left(S_{oy} - S_{fy}\right) \quad (2)$$

where $u^L{}_i$ = x-component velocity, $v^L{}_i$ = y-component velocity, S_o = bottom elevation, g = gravitational acceleration, $S_f = c_f\, u_i\, |u_i|/(2gh)$ = friction slope, and c_f = coefficient of bottom friction. In the Lagrangian reference frame, the position $x^L{}_i(t)$ and the velocities $u^L{}_i(t)$ and $v^L{}_i(t)$ are functions of time only. A numerical solution is possible when the Courant number Co = $\max[u\Delta t/\Delta x, v\Delta t/\Delta y]$ is less than unity. This Courant stability condition is the only condition needed for a successful LBH computation.

3 COMPUTATIONAL STABILITY AND ACCURACY

The most significant advantage of the LBH over other computation methods is the computational stability. Besides the usual Courant stability requirement, LBH computation is absolutely stable. The method is also accurate. Grid refinement studies have been carried out previously by Tan and Chu (2009a,b) to show the convergent of the 1D LBH computations toward the exact solutions. Validation of the computations has been obtained for the dam-break flood waves by Ritter (1892), Stoker (1957), Hogg (2006), Ancey et al. (2008), and for the runup and overtopping of the collapsing bores by Shen and Meyer (1963) and Peregrine and Williams (2001).

The computational stability and accuracy of the LBH is further demonstrated in this paper by the following 2D examples that have exact solutions.

3.1 *Oblique Dam-Break Waves*

The first example is the oblique dam-break shock wave in a 100 m × 100 m square basin. The initial water depth upstream is h_o = 10 m and the downstream water depth h_d = 1 m. The removal of a dam along the diagonal of the basin causes the water on the upstream to advance on a wet bed. Figures 2(a)-2(c) show depth contours obtained by the LBH computation for time t = 0.1 s, 2.5 s and 4.0 s, respectively. Figures 2(d) and 2(e) compare the depth and velocity profiles computed by the LBH method. The circles denote the exact solution of Stoker (1957). The LBH computation is denoted by the solid line. The exact solution h_s/h_o = 0.396 is accurately captured without using any shock capturing scheme. Figure 2(f) shows the

convergence towards the exact solution as the block is refined follows the first-order accuracy in the sense of Celik et al. (2008).

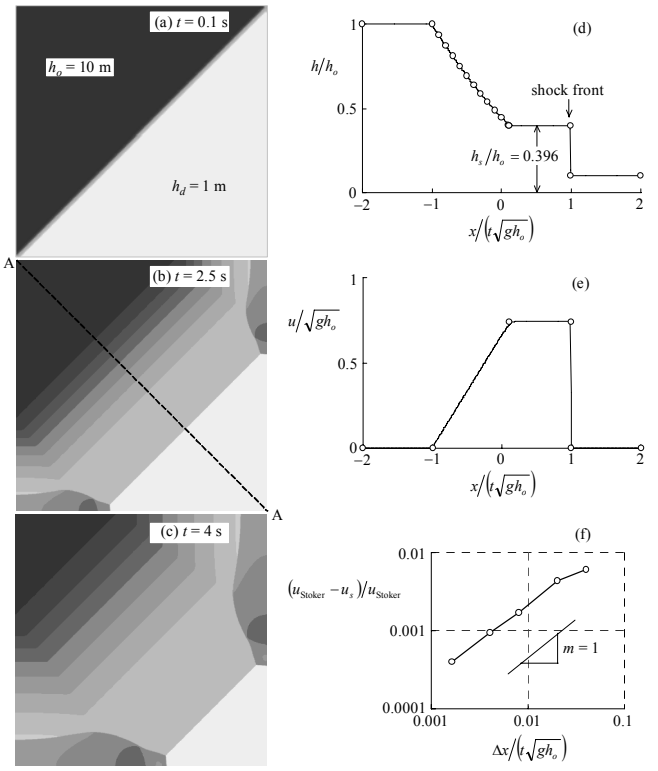

Figure 2. (a-c) Simulated water depth contours of oblique dam-break waves on wet downstream depth using mesh size Δx = 0.04 m, (d-e) cross-sectional profile A-A at time t = 2.5 s, (f) LBH convergence towards Stoker (1957) solution.

3.2 *Standing Waves in Parabolic Bowl*

Figure 3 shows the 2D LBH computation of the standing wave in a parabolic bowl. The motion is initiated by a parabolic mound of water. The wetting and drying on the surface of the bowl is a challenging numerical computation. At the wave front, numerical oscillations can produce negative water depth, and subsequently lead to computation breakdown. The 2D LBH has been able to simulate infinite number of cycles of flow oscillations as the water advances and recesses on the surface of the parabolic bowl without any sign of numerical instability.

4 CONCEPTUAL RIVER-FLOW MODEL

The capability (i) to track the advancing-and-retreating fronts on dry bed and (ii) to capture the depth-and-velocity discontinuity across the shock waves, has made the 2D LBH an ideal computational method for the routing of the high-speed flood waves in steep river channel. Simulations are conducted to demonstrate the capability of the method using a conceptual river-flow model as shown in Fig. 4. The width and length of the computational channel are B and L, respectively. An array of spur dikes lines the side of the channel.

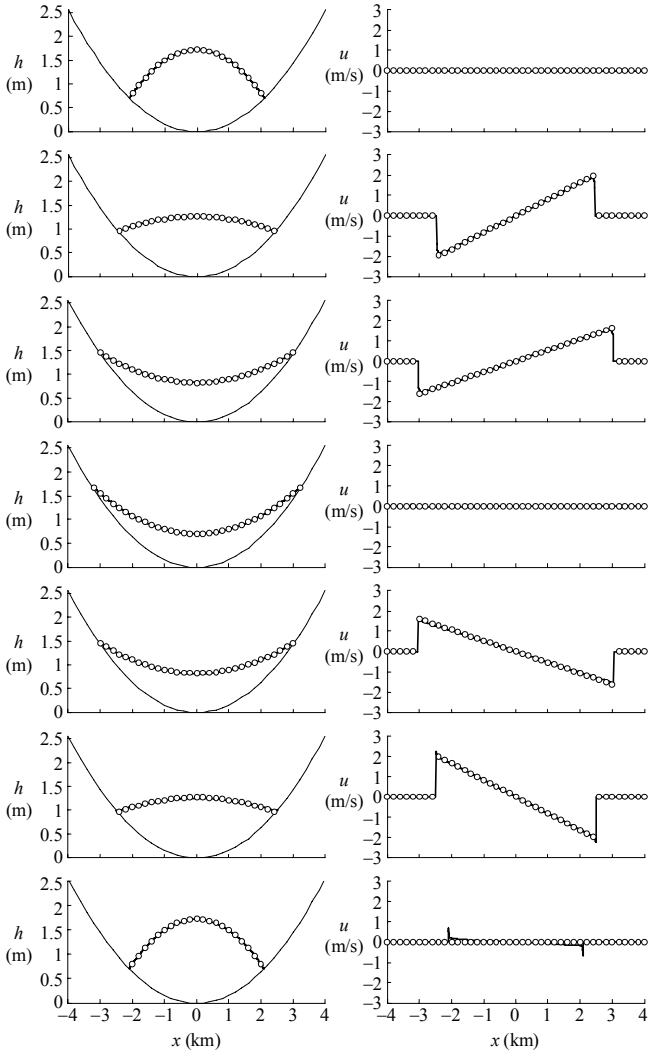

Figure 3. Water depth h and velocity u in the parabolic bowl of an initial 2 km radius as computed by the block advection using $\Delta x = \Delta y$ = 5 m are shown at a time interval of one-sixth cycle. The computed profiles on the plane of symmetry y = 0 are the solid line. The exact solution of Thacker (1981) is denoted by the circle symbol.

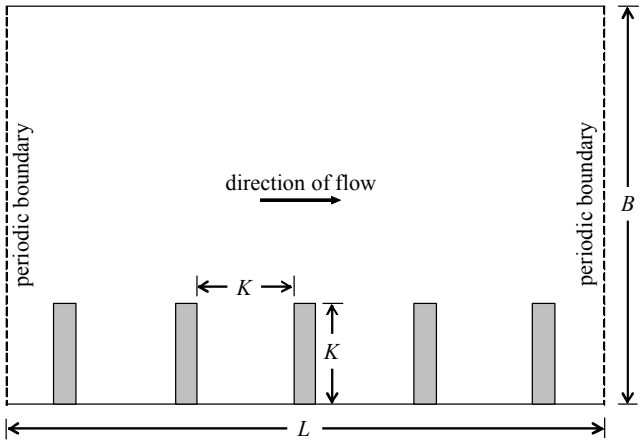

Figure 4. Conceptual river-flow model for LBH simulation. The macro resistance is produced by lateral exchanges of fluids between the main flow and the array of shoreline features.

The basins between the dikes are squares. The dimension of the square basins, K, is the only

length scale that characterizes the macro resistance. The flow is repeated over the length L using the periodic boundary conditions. This highly idealized river-flow model is designed for ease of computation and the generalization of the computation results.

4.1 *Flood Water into Dry Cavities*

The advance of flood water into dry cavity is the first flood routing problem computed by LBH using the conceptual river-flow model. Figure 5 shows the water depth and vorticity profiles of the river over a period of time. The initial water depth in the main channel is h_o = 6 m and the initial velocity is U_o = 10 m/s. The basins are initially dry. The flow in the main channel is supercritical with a Froude number Fr = 1.30. Despite the high speed of the supercritical flow, the LBH has been able to simulate the advance of the water into the dry basins with absolute computational stability.

4.2 *Macro Flow Resistance*

The resistance to the flow on the one hand is dependent on the bottom friction coefficient c_f. It also is dependent on the macro resistance produced by the channel features such as the flood plains, spur dikes and bends along the channel.

The "macro resistance" to flow depends on the size and shape of the "macro roughness" and has to be determined case by case by calculating the flow around the macro roughness. The real river channels however are variable in space and time due to erosion and deposition of sediments along the channel (Web et al. 1999). A reliable computational model should be able to determine not only the flow but also the morphological changes to the channel.

To demonstrate the existence of macro resistance, LBH simulations have been conducted for the conceptual river-flow channel. The Reynolds stresses at the junction between the macro roughness and the main channel flow has been computed and correlated with two dimensionless parameters: bed-friction number $S = c_f K/h$ and Froude number Fr = $U/(gh)^{1/2}$. The bed-friction number characterizes the effect of the bottom friction and the Froude number on the effect of gravity-wave radiation. Both the bed-friction and the radiation of waves can have significant effect on the shear instabilities as demonstrated by the stability analysis by Pinilla and Chu (2008, 2009a,b).

The LBH simulations of the waves and turbulence around the macro roughness in the conceptual river-flow channel has been carried out for two water depths h_o = 1 cm and 6 cm, two channel slopes S_o = 0.1 and 0.01 and a range of different bottom friction coefficients c_f = 0, 0.08 and 0.008.

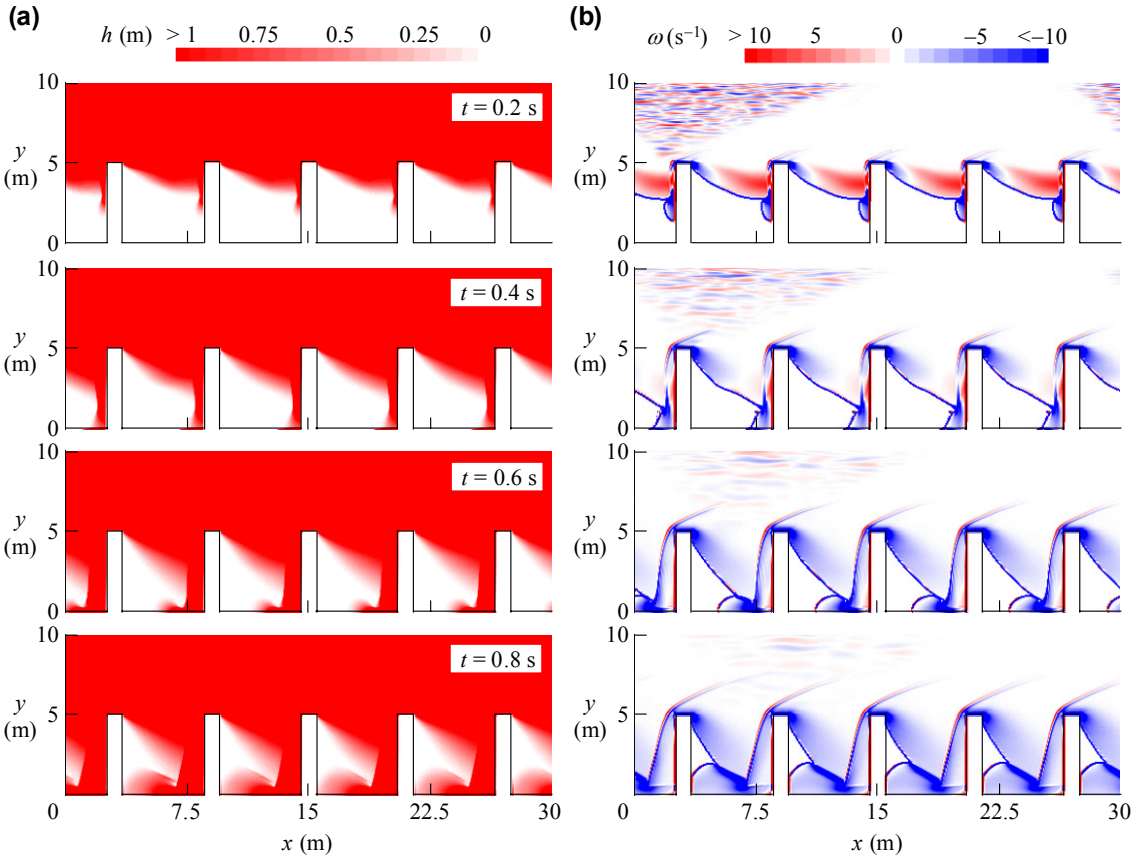

Figure 5. Advance of flood waters onto the dry cavities at time t = 0.2 s to 0.8 s; (a) water depth h and (b) vorticity ω profiles of the flow of initial water depth h_o = 6 m, initial velocity U_o = 10 m/s and initial Froude number Fr = 1.30; the bed slope S_o = 0.1, the bottom friction coefficient c_f = 0 and macro roughness K = 5 m.

The bed-friction number varies over the range from $S = 0$ to 0.413. The Froude number varies over the range from Fr = 0.45 to 6.62. Table 1 summarizes the conditions of the simulations.

Figures 6 and 7 show the dilation and vorticity profiles obtained by LBH for two of the simulations. One is for the flow on a mild slope with $S_o = 0.01$, Fr = 1.06 and the other on a steep slope with $S_o = 0.1$, Fr = 2.68. Besides the coherent turbulence, the breaking gravity waves are observed and have played a significant role in determining the macro resistance in both of these simulations. Breaking waves in the form of shock waves are observed in the supercritical flow with the high Froude number.

4.3 *Lateral Resistance Coefficient*

Once the flow velocity is computed, it is divided into mean and fluctuating parts: $u = U + u'$, $v = V + v'$. The lateral exchanges of the momentum $-\rho\langle u'u'\rangle$, $-\rho\langle u'v\rangle$, and $-\rho\langle v'v'\rangle$ are evaluated subsequently. The exchange at the junction between the cavities and the main flow where $y = K$ determines the lateral resistance coefficient C_{LR}, which is as follow:

$$C_{LR} = \frac{-\rho\langle u'v'\rangle_{y=K}}{\frac{1}{2}\rho U^2} = -2\frac{\langle u'v'\rangle_{y=K}}{U^2} \tag{3}$$

where $-\rho\langle u'v'\rangle_{y=K}$ = Reynolds stresses obtained by averaging along the flow at the junction where $y = K$, and U = mean velocity of the main flow.

Table 1. LBH simulations for subcritical and supercritical flows with $B = 20$ cm and $K = 5$ cm

h_o (cm)	S_o	c_f	U_{QS} (cm/s)	Fr	$S = c_f k/h_o$	C_{LR}
1	0.01	0	65.11	2.09	0	0.060
1	0.01	0.008	39.82	1.28	0.041	0.056
1	0.01	0.080	15.12	0.49	0.413	0.024
1	0.1	0	207.61	6.62	0	0.011
1	0.1	0.008	128.36	4.08	0.040	0.046
1	0.1	0.080	48.19	1.55	0.408	0.042
6	0.01	0	80.66	1.06	0	0.018
6	0.01	0.008	65.95	0.87	0.007	0.020
6	0.01	0.080	34.04	0.45	0.068	0.030
6	0.1	0	204.13	2.68	0	0.069
6	0.1	0.008	183.20	2.41	0.007	0.072
6	0.1	0.080	106.81	1.40	0.068	0.055

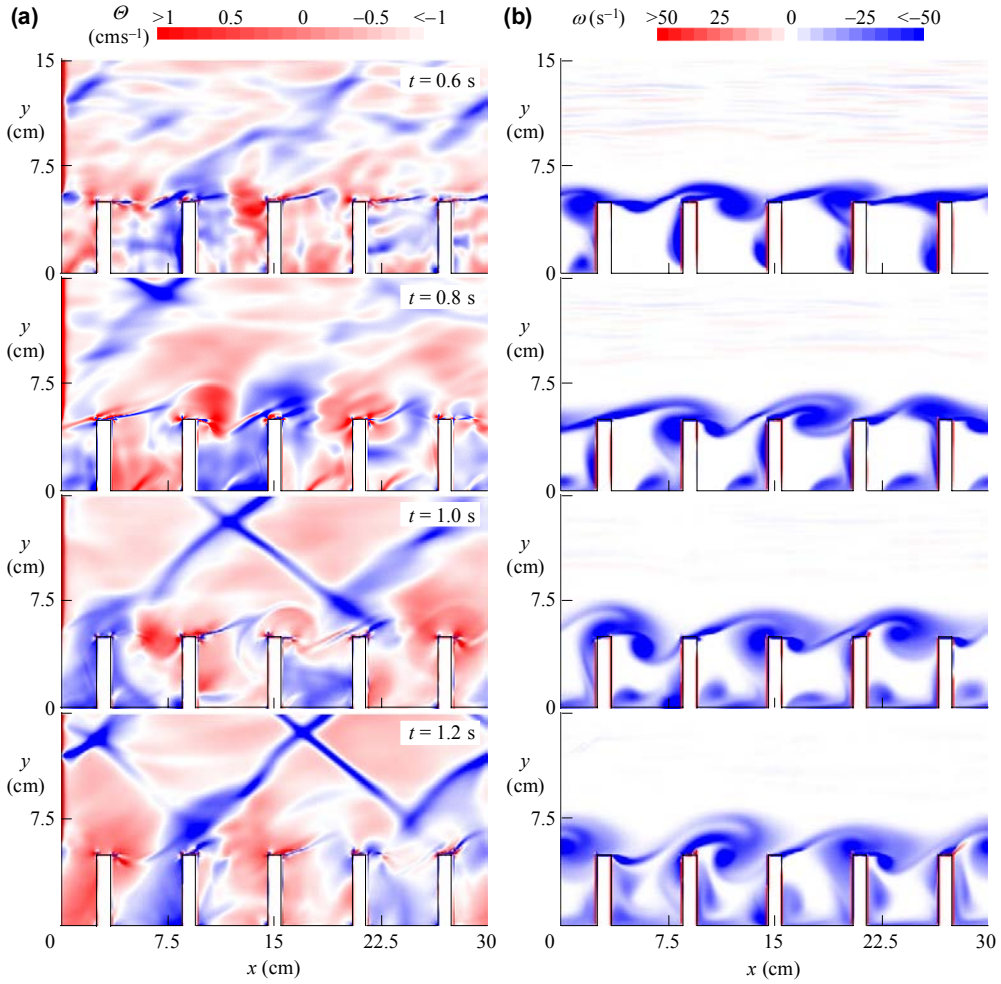

Figure 6. Dilation Θ and vorticity ω profiles for the river flow of water depth $h_o = 6$ cm, slope $S_o = 0.01$, bottom friction coefficient $c_f = 0$, and Froude number Fr = 1.06.

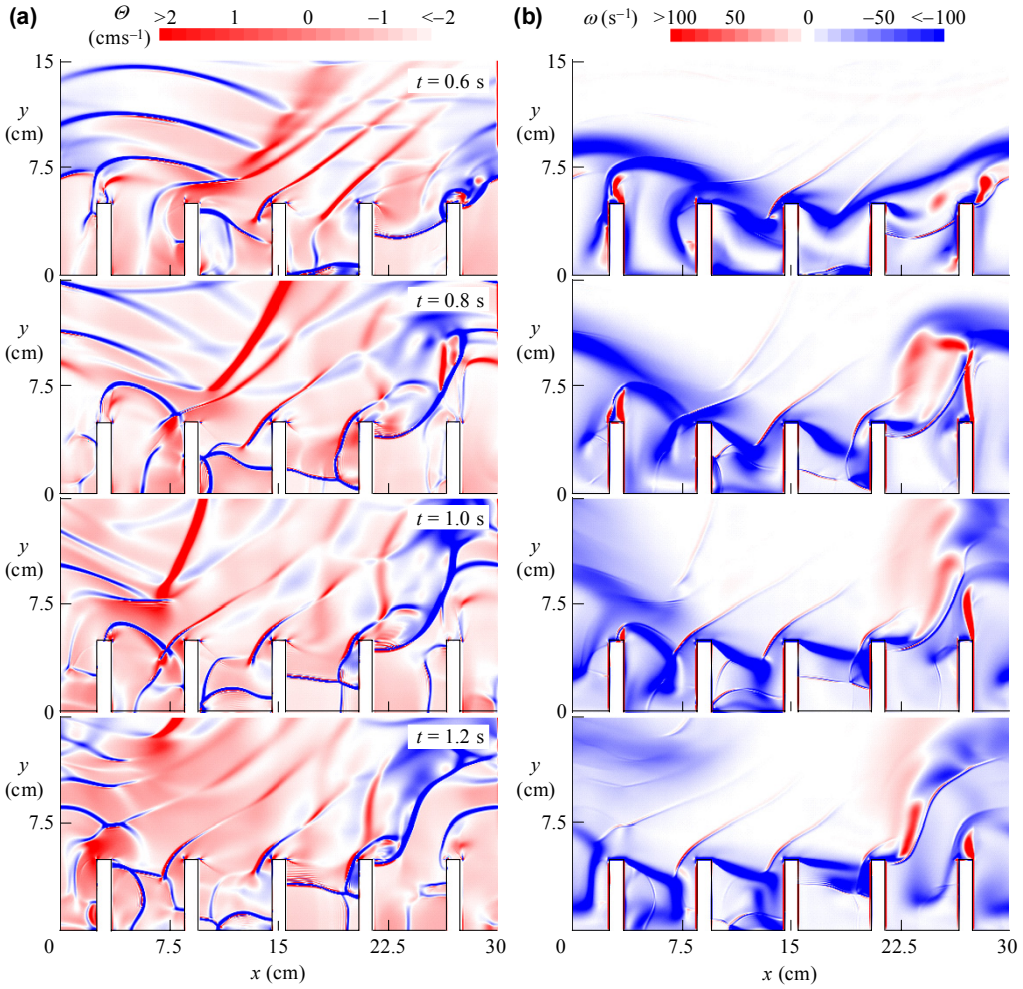

Figure 7. Dilation Θ and vorticity ω profiles for river flow of water depth h_o = 6 cm, slope S_o = 0.1, coefficient of friction c_f = 0, and Froude number Fr = 2.68.

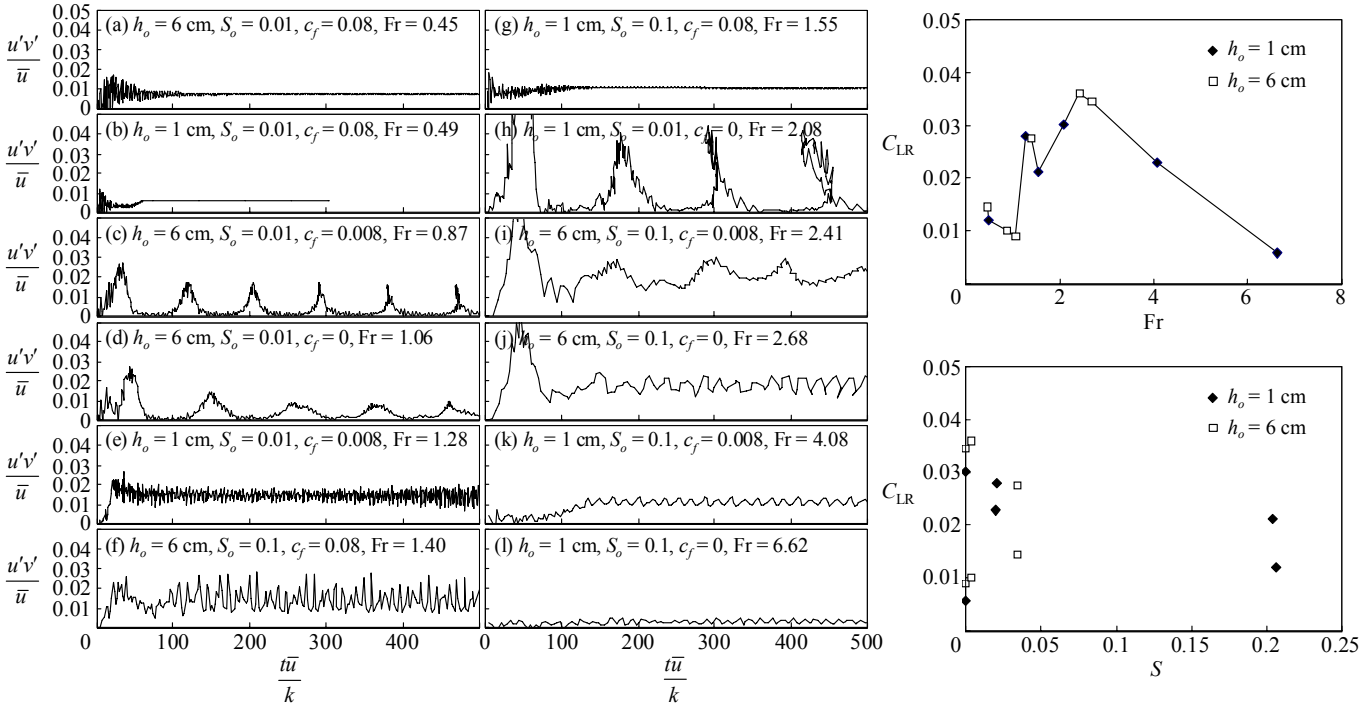

Figure 8. (a-l) Reynolds stresses $\langle u'v' \rangle / U^2$ obtained for flows in ascending order of Froude number, (m) lateral resistance coefficient C_{LR} dependence on Froude number Fr, and (n) later resistance coefficient C_{LR} dependence on bed-friction number S.

The Reynolds stresses and the lateral exchange coefficients obtained from the presented series of simulations are correlated with the bed-friction number and the Froude number. These correlations are shown in Fig. 8. Since the macro roughness is large compared with the width of the channel in these simulation, the strong dependence on the Froude number is expected. The radiation of waves from the shear flow may explain why the significance of the Froude number on the exchanges.

5 CONCLUSIONS

The tracking of flood waves on dry land and the capture of the depth-and-velocity discontinuities across the breaking waves has been carried out by the Lagrangian block hydrodynamics (LBH) with absolute computational stability. The phenomenon of the lateral exchanges due to macro roughness is complex. The results in this paper show only the capability of the LBH method. Nevertheless, the simulations have suggested how the method can deal with flood routing problems of even greater complexity.

The stability of the method is an advantage over other computation methods in negotiating waters through the complex bathymetry in steep channel flows. The LBH method is also accurate as demonstrated in the simulations of (i) the advancing-and-retreating front over the dry bed in a parabolic bowl, and (ii) the oblique shock waves in the square basin and their comparison with the exact solutions in this paper. Not only the method is successful in the simulation of surface water waves the method is also capable of simulating turbulent flows. The results presented in this paper have shown how turbulence is simulated around the macro roughness so that the lateral resistance of the roughness in both the subcritical and supercritical turbulent shear flows is computed by LBH.

Laboratory investigation is part of the overall project to study the lateral exchanges in steep channel flow of complex geometry. The analysis of the laboratory data has not been completed. However, the numerical simulations of the flows are available. Figure 9 shows one of the simulation results carried out for the conditions of the flow and the dimensions of the channel in one of the laboratory experiment. Qualitative agreement between simulation and laboratory has been observed. The quantitative verification of the LBH model against the laboratory data should be ready by the time this paper is presented in the conference.

REFERENCES

Ancey, C., Iverson, R.M., Rentschler, M., Denlinger, R.P. 2008. An exact solution for ideal dam-break floods on steep slopes. Water Resources Research, 44, W01430.

Celik, I.B., Ghia, U., Roache, P.J., Freitas, C.J., Coleman, H., Raad, P.E. 2008. Procedure for estimation and reporting of uncertainty due to discretization in CFD applications. Journal of Fluids Engineering, 130, 1-4.

Chu, V.H., Altai, W. 2001. Simulation of shallow transverse shear flow by generalized second moment method. Journal of Hydraulic Research, 39(6), 575-582.

Chu, V.H., Altai, W. 2002. Simulation of turbulence and gravity interfaces by Lagrangian block method. Computational Fluid Dynamics 2002, New York: Springer-Verlag, 299-304.

Harlow, F.H. 1964. The particle-in-cell computing method for fluid dynamics. Methods in Computational Physics, 3, 319-343.

Hogg, A.J. 2006. Lock-release gravity currents and dam-break flows. Journal of Fluid Mechanics, 569(1), 61-87.

Monaghan, J.J. 2005. Smoothed particle hydrodynamics. Reports on Progress in Physics, 68(8), 1703-1759.

Peregrine, D.H., Williams, S.M. 2001. Swash overtopping a truncated plane beach. Journal of Fluid Mechanics, 440, 391-399.

Pinilla, C. and Chu, V.H. (2008) "Waves and Bed-Friction Effect on Stability of Transverse Sheer Flow in Shallow Waters," Journal of Coastal Research, Vol. S52, ISSN 0749-0208, pp. 207-214.

Pinilla, C.E. and Chu, V.H. (2009a) "The Role of Wave Radiation on Instability of Coastal Current," Proc. 33rd Congress of IAHR, ISBN 978-90-78046-08-0, Aug 9-14, Vancouver, Canada, 8 pp. in CD ROM.

Pinilla, C.E. and Chu, V.H. (2009b) "Wave radiation and shear instability in rotating stratified flow," *Proc. 28th Int. Conf. on Ocean, Offshore, and Arctic Eng.*, ISBN 978-0-7918-3844-0, May 31- June 5, Honolulu, Hawaii, ASME paper OMAE2009-79416, 8 pp.

Ritter, A. 1892. The propagation of water waves. Zeitschrift des Vereines Deutsher Ingenieure, 36(33), 947-954.

Webb, R.H., Schmidt, J.C., Marzolf, G.R., and Valdes, R.A. editors. 1999. The Controlled Flood in Grand Canyon. Geophysical Monograph 110, American Geophysical Union, 367 pp.

Shen, M.C., Meyer, R.E. 1963. Climb of a bore on a beach: part 3, run-up. Journal of Fluid Mechanics, 16(1), 113-125.

Stoker, J.J. 1957. Water Waves: The Mathematical Theory with Applications. Wiley Interscience.

Tan, L.W., Chu, V.H. 2009a. Simulation of wave fronts on dry beds using Lagrangian blocks. Engineering and Computational Mechanics, 162(EM2), 57-66.

Tan, L.W., Chu, V.H. 2009b. Lauber and Hager's dam-break wave data for numerical model validation. Journal of Hydraulic Research, 47(4), 524-528.

Tan, L.W., Chu, V.H. 2010. Wave runup simulations using Lagrangian blocks on Eulerian mesh. Journal of Hydro-environment Research, 3(4), 193-200.

Thacker, C.W. 1981. Some exact solutions to the nonlinear shallow-water wave equations. Journal of Fluid Mechanics, 107, 499-508.

AGU Monograph 110, 1999. The Controlled Floods in Grand Canyon. Geophysical Monograph 110, Webb, R.H., Schmidt, J.C., Marzolf, G.R. and Valdez, R.A. editors, American Geophysical Union, Washington, D.C., 367 pp.

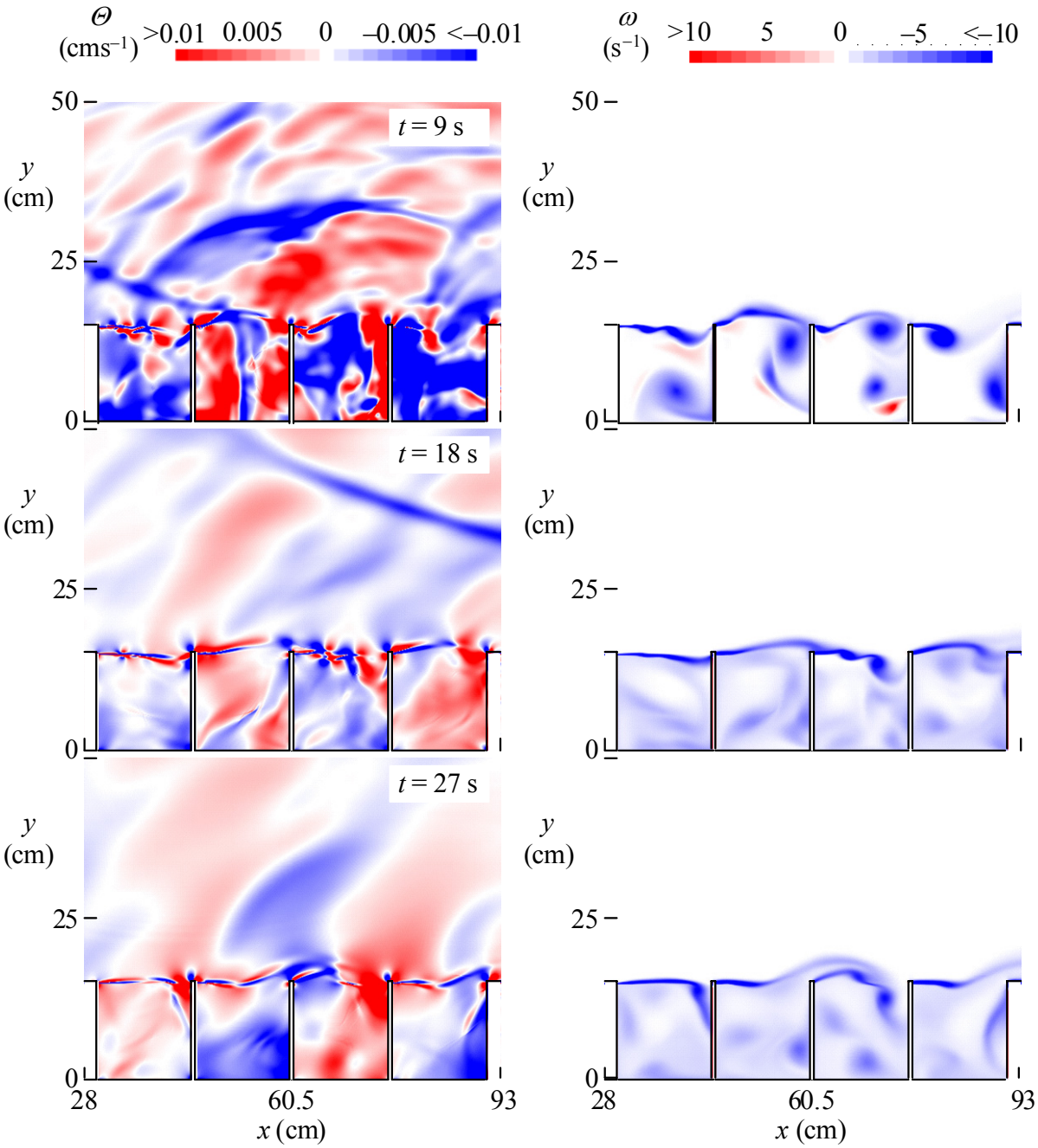

Figure 9. Dilation Θ and vorticity ω profiles for the channel flow of water depth h_o = 0.69 cm, slope S_o = 0.0001, coefficient of friction c_f = 0.008, and Froude number Fr = 0.55. The width of the main open-channel flow is 1.41 m. The dimension of the square basin on the side of the main channel flow is 0.45 m.